Predictions of scanning tunneling microscope images of furan and pyrrole on Pd(111)

D. N. Futaba[a] and S. Chiang[b]
Department of Physics, University of California, Davis, California 95616

(Received 14 October 1996; accepted 31 March 1997)

We use a computational method, based on extended Hückel molecular orbital theory, for predicting the scanning tunneling microscope images of furan and pyrrole adsorbed onto Pd(111). We calculated images for both isolated molecules and for molecules chemisorbed onto a metal cluster. From binding energy calculations, the low energy geometries for three binding sites were determined. We found many similarities between furan and pyrrole in the preferred binding site geometries and images. © *1997 American Vacuum Society.* [S0734-2101(97)60903-3]

I. INTRODUCTION

Understanding heterogeneous catalysis is important for the production and refinement of petroleum fuels. However, there is currently little molecular understanding of the catalysis of heterocompounds, such as furan and pyrrole, on metals. Therefore, the relationship between the surface structure and the surface reactivity for such compounds on late transition metals, such as Pd, is important for understanding the use of these metals as promoters to remove the O and N heteroatoms from these molecules. Thus, we plan to conduct variable temperature scanning tunneling microscope (STM) studies of the decomposition of furan and pyrrole on Pd(111). As preparation for those experiments, we have calculated the predicted images for furan and pyrrole on Pd(111) using extended Hückel theory (EHT).

II. METHOD

Though limited to aromatic molecules, a method[1,2] for predicting STM images based on EHT has been successful in reproducing the detailed internal structures of such carbon-ring structures as naphthalene, azulene, monomethylazulene, dimethylazulene, and trimethylazulene on Pt(111). The EHT treatment of conjugated hydrocarbons is a semiempirical calculation which combines linear combination of atomic orbitals (LCAO), the variational method, and matrix mechanics. The total wave function is represented as a linear combination of Slater-type atomic orbitals of all the valence electrons in the system. By minimizing the total energy with respect to each coefficient, the contributions from the atomic orbitals to the complete molecular orbital(s) for an isolated molecule or for a molecule adsorbed onto a metal cluster are computed. No other energy minimization or molecular relaxation was performed. Parameters for Pd were taken from the literature[3,4] and are listed in Table I.

Unless information is known as to the binding site and orientation of the molecule with respect to the cluster, the binding energy is calculated and plotted as a function of molecular-cluster separation for each configuration to find the low energy geometry. The molecule-cluster separation is determined by the location of the minimum in the binding energy curve.

According to the Tersoff–Hamann theory of operation of the STM,[5] the tunneling current is proportional to the surface local density of states (LDOSs) evaluated at the Fermi level at the height of the tip. For the isolated molecules, we plot 15 Å×15 Å images of the highest occupied molecular orbital (HOMO) and the lowest unoccupied molecular orbital (LUMO). Experimentally, these correspond to the negative and positive sample bias settings of an STM. The LDOS is evaluated at different tip heights to correspond to variable image resolution.

Because the tip does not tunnel to a single orbital as a result of the bias voltage, an energy integration is performed to include all molecular orbitals within a 1 eV window above or below the Fermi level. The energy integration also insures that the images include molecular character which is not found only in the HOMO or LUMO due to the hybridization with metal orbitals near the Fermi level. It is these occupied and unoccupied states that are then plotted for the adsorbed cases. The base ten logarithm of the calculated images is taken so as to correspond better to constant current experimental STM images. Finally, the images were convolved with a Gaussian of 1 Å full width at half-maximum (FWHM) to correct for finite size tip effects.

These programs have been successfully ported from an IBM mainframe computer to a 150 MHz Pentium-based PC. In our study, the Pd metal clusters consisted of a single hexagonal layer of ~20 atoms. Computation of the energy eigenvalues took approximately 2–5 min. Another 2–5 min were needed to generate both occupied and unoccupied state images.

III. RESULTS AND DISCUSSION

Figure 1(a) is a schematic diagram of furan and pyrrole. Note the similarity in shape. Figure 1(b) shows the resultant low energy binding sites and orientations from the binding energy calculations. Figure 2 shows binding energy plots for furan adsorbed onto Pd(111). The binding energy computations found no discernible preference between the 0° and 90° orientations of furan for the on-top site. In fact, since the

[a]Electronic mail: dfutaba@landau.ucdavis.edu
[b]Author to whom all correspondence should be addressed; Electronic mail: chiang@physics.ucdavis.edu

TABLE I. Palladium EHT parameters.

Orbital	Valence orbital ionization potential (eV)	Slater exponent
4*d*	−12.02	5.983(0.5534)
		2.613(0.6701)
5*s*	−7.32	2.190
5*p*	−3.45	2.152

images for the two on-top sites were virtually identical except for the 90° rotation, we show only the 0° case in this article. Furan in three-fold hollow sites slightly favors the 180° orientation shown in Fig. 1(b). Finally, we found that furan on bridge sites aligns its symmetry axis perpendicular to the bridge. Of the three binding sites, the binding energy curves indicate that the bridge site at 0° is the most energetically favorable geometry.

Pyrrole showed the same geometrical tendencies on the Pd cluster, except that the orientation with the 90° rotation was slightly favored for the on-top binding site and the two hollow sites have nearly the same energies. As with furan, pyrrole also favors the bridge site over all binding sites tested.

Figure 3 is a set of the predicted images corresponding to the configurations for furan on a Pd(111) cluster. The two columns are images for the same binding site but at different tip heights. We can extract more detailed structural information from images with the LDOS calculated closer to the molecular plane, which correspond to higher resolution STM images as expected. Figures 3(a) and 3(b) are the HOMOs for the isolated molecule at two different heights above the surface. We speculate that the strong electron density adjacent to the oxygen atom is due to the dipole moment of furan. In the top site occupied state images [Figs. 3(c) and 3(d)], we can see how the cluster affects the image of furan. The effects are more noticeable in the image where the LDOS was calculated at a smaller distance from the molecular plane. The hollow site images in Figs. 3(e) and 3(f) show a remarkable similarity to the isolated case. Furthermore, the bridge site images [Figs. 3(g) and 3(h)] also show resemblance to isolate furan, but with additional features.

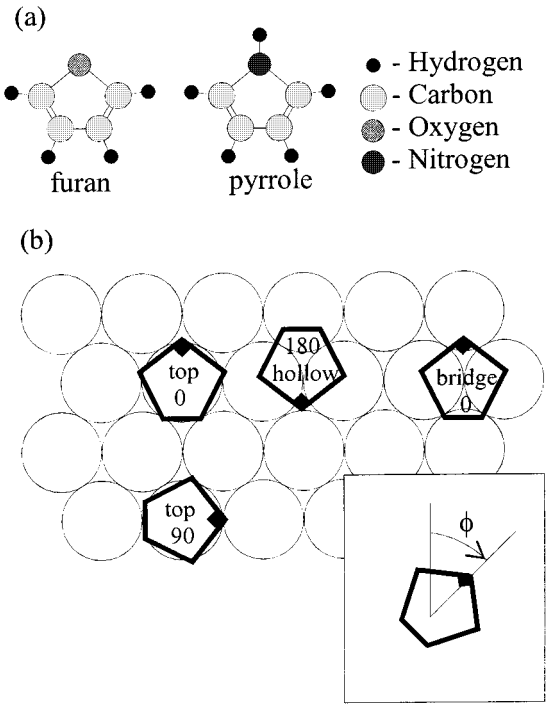

FIG. 1. (a) Schematic diagram of furan and pyrrole. (b) The low energy adsorption geometries of furan and pyrrole on Pd(111) for the high symmetry binding sites: on-top, three-fold hollow, and bridge sites. The numerals indicate the rotation angle in degrees, ϕ, of the heteroatom as shown in the inset.

Figure 4 shows the images for the low energy geometries of pyrrole. Figures 4(a) and 4(b) show the HOMOs for the isolated molecule at two different heights above the surface. As with furan, we attribute the strong electron density adjacent to the nitrogen atom to its dipole moment. Figures 4(c) and 4(d) show the molecule with a four-lobe feature much

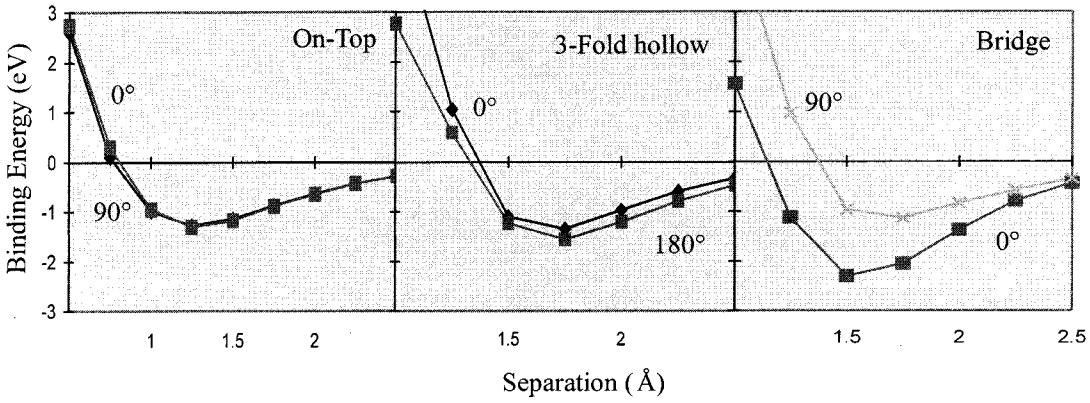

FIG. 2. Binding energy curves for furan adsorbed onto Pd(111). Three different binding sites were investigated: on-top, bridge, and three-fold hollow. Different symbols indicate the azimuthal orientation of the molecule with respect to the lattice, as indicated in Fig. 1(b).

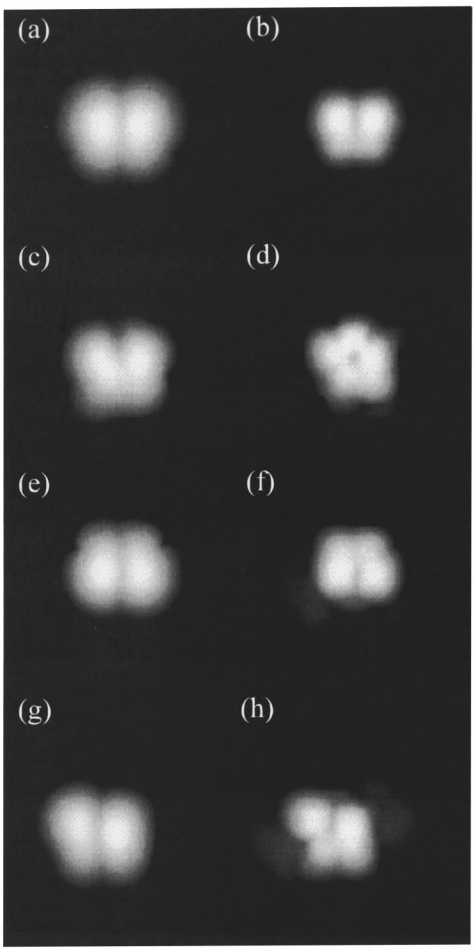

FIG. 3. Furan on Pd(111) cluster. HOMO for isolated furan rotated 0° at (a) 2 Å above the molecular plane and at (b) 0.5 Å. Occupied states for on-top site rotated 0° at (c) 2 Å and at (d) 0.5 Å; three-fold hollow site rotated 180° at (e) 2 Å and at (f) 0.5 Å; Bridge site rotated at 0° at (g) 2 Å and at (h) 0.5 Å.

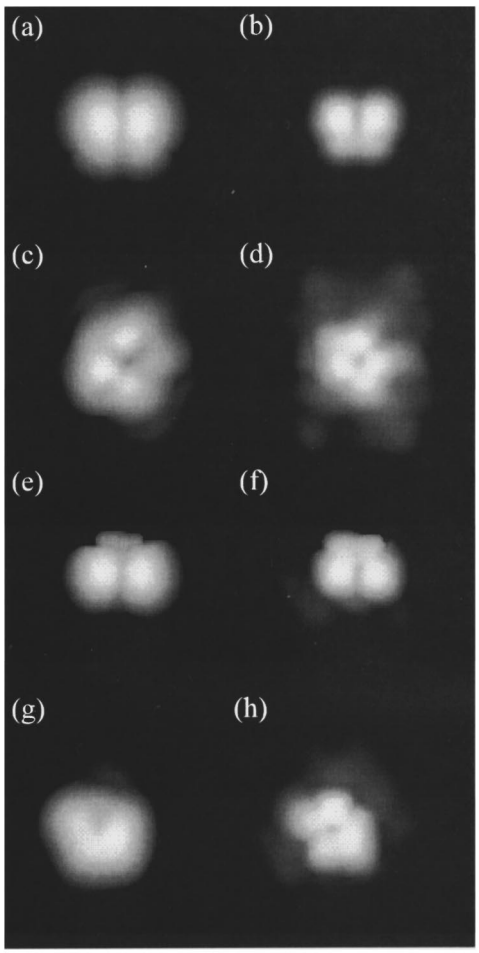

FIG. 4. Pyrrole on Pd(111) cluster. HOMO for isolated pyrrole rotated 0° at (a) 2 Å above the molecular plane and at (b) 0.5 Å. Occupied states for on-top site rotated at 90° at (c) 2 Å and at (d) 0.5 Å; three-fold hollow site rotated at 180° at (e) 2 Å and at (f) 0.5 Å; Bridge site rotated 0° at (g) 2 Å and at (h) 0.5 Å.

different than that of furan on the same site. As a result of the smaller equilibrium molecular-cluster separation for pyrrole compared to furan, we expect the molecular orbitals to be more strongly hybridized with those of the metal, leading to less distinguishable molecular features. The three-fold hollow site images of Figs. 4(e) and 4(f) show strong resemblance to isolated pyrrole with exceptionally strong electron densities adjacent to the nitrogen atom. While the images of pyrrole on bridge sites [Figs. 4(g) and 4(h)] show some similarity to images of furan on the same site [Figs. 3(g) and 3(h)], they bare little resemblance to the images of pyrrole on the other sites.

The experimental images for the bridge site, however, may be quite different from those calculated here if the sample-tip effects from Sautet *et al.*'s calculations for benzene on Pt(111) apply here.[6] Experimentally, benzene on a Pt(111) bridge site demonstrated a single bump feature,[7] which was attributed to interference between the tunneling current through the molecule and directly from the metal.[6] Apparently, the interference was constructive in the center and destructive outside the carbon ring, resulting in convolving a two peak image to a simple peak. The other binding sites showed these effects to a much lesser degree. Thus, for the EHT calculations shown here, our assumption that the images are a result from current through the molecule only is probably reasonable for the on-top and three-fold hollow sites.

IV. SUMMARY

Predicted STM images were presented for furan and pyrrole on Pd(111) using EHT as the basis for the calculations. We expect the bridge site to be the most probable binding site from energy calculations. However, all three binding sites may be possible for low temperature physisorbed or chemisorbed molecules as for benzene on Pt(111) at 4 K.[7] Because of the characteristic features in the predicted images for pyrrole, we expect to be able to distinguish between molecules adsorbed onto these different binding sites. The same

cannot be said for furan, but we expect to be able to differentiate between the two molecules if mixed on the same surface.

ACKNOWLEDGMENTS

The authors acknowledge Quantum Chemistry Program Exchange (QCPE) for the program FORTICON 8. They also gratefully thank V. M. Hallmark, T. E. Caldwell, G. W. Anderson, and B. Lau for their helpful discussions. This work was supported by the National Science Foundation under Grant No. CHE-95-20366 and by the Campus Laboratory Collaborations Program of the University of California.

[1]V. M. Hallmark and S. Chiang, Surf. Sci. **329**, 255 (1995).
[2]V. M. Hallmark, S. Chiang, K.-P. Meinhardt, and K. Hafner, Phys. Rev. Lett. **70**, 3740 (1993).
[3]V. S. Gurin and A. B. Kovrikov, Appl. Surf. Sci. **81**, 43 (1994).
[4]E. Clementi and C. Roetti, At. Data Nucl. Data Tables **14**, 177 (1974).
[5]J. Tersoff and D. R. Hamann, Phys. Rev. Lett. **50**, 1998 (1983).
[6]P. Sautet and M.-L. Bocquet, Phys. Rev. B **53**, 4910 (1996).
[7]P. S. Weiss and D. M. Eigler, Phys. Rev. Lett. **71**, 3139 (1993).